Unimolecular Dissociations of C_{70}^+ and Its Noble Gas Endohedral Cations $Ne@C_{70}^+$ and $Ar@C_{70}^+$: Cage-Binding Energies for C_2 Loss

Baopeng Cao,*,†,‡ Tikva Peres,‡ R. James Cross,*,# Martin Saunders,# and Chava Lifshitz‡,¶

Department of Physical Chemistry and The Farkas Center for Light Induced Process, The Hebrew University of Jerusalem, Jerusalem 91904, Israel, Department of Chemistry, Indiana University, 800 East Kirkwood Avenue, Bloomington, Indiana 47404, and Department of Chemistry, Yale University, New Haven, Connecticut 06520-8170

Received: August 24, 2005; In Final Form: September 16, 2005

The energetics and dynamics of unimolecular decompositions of C_{70}^+ and its noble gas endohedral cations, $Ne@C_{70}^+$ and $Ar@C_{70}^+$, have been studied using tandem mass spectrometry techniques. The high-resolution mass-analyzed ion kinetic energy (HR-MIKE) spectra for the unimolecular reactions of C_{70}^+, $Ne@C_{70}^+$, and $Ar@C_{70}^+$ were recorded by scanning the electrostatic analyzer and using single-ion counting that was achieved by combination of an electron multiplier, amplifier/discriminator, and multichannel analyzer. These cations dissociate unimolecularly via loss of a C_2 unit, and no endohedral atom is observed as fragment. The activation energies for C_2 evaporation from $Ne@C_{70}^+$ and $Ar@C_{70}^+$ are lower than those for elimination of the endohedral noble gas atoms. The kinetic energy release distributions (KERDs) for the C_2 evaporation have been measured and, by use of the finite heat bath theory (FHBT), the binding energies for the C_2 emission have been deduced from the KERDs. The C_2 evaporation energies increase in the order $\Delta E_{vap}(C_{70}^+) < \Delta E_{vap}(Ne@C_{70}^+) < \Delta E_{vap}(Ar@C_{70}^+)$, but no big difference in the cage binding was observed for C_{70}^+, $Ne@C_{70}^+$, and $Ar@C_{70}^+$, indicating incorporations of the Ne and Ar atoms into C_{70} contribute a little to the stability of C_{70} toward C_2 loss, which is in good agreement with theoretical calculations but contrasts with the findings in their C_{60} analogues and in metallofullerenes that the decay energies of the filled fullerenes are much higher than those of the corresponding empty cages.

1. Introduction

Evidence that noble gas atoms can be encaged inside the hollow space of C_{60}^+ and C_{70}^+ was first found by Schwarz and co-workers through high-energy collision experiments.[1] Endohedral fullerenes with a noble gas atom inside are prepared by heating the fullerenes under high pressure of the noble gas.[2] The typical yield for rare gas endohedral fullerenes thus produced is around 0.1%. To elucidate the encapsulation of noble gas atoms inside fullerenes, a mechanism for incorporation and release of the guest atom was proposed involving reversibly breaking a bond to open a window in the cage.[3] Neutral molecules or atoms such as He, Ne, Ar, Kr, Xe, N, N_2, H_2, CO, H_2O, and HeNe have thus far been doped inside C_{60}.[4−7] $N@C_{70}$ and $N_2@C_{70}$ have been synthesized by ion implantation as well.[6c,7]

It would be of interest to know if the two most abundant fullerenes, C_{60} and C_{70}, are stabilized upon introduction of the noble gases into their hollow spaces. The stabilization energy $E_{cmplx}(Rg@C_n)$, also termed as complexation, binding, or embedding energy of endohedral fullerene $Rg@C_n$, is defined as follows:[8]

$$Rg + C_n \rightarrow Rg@C_n \qquad E_{cmplx}(Rg@C_n) \qquad (1)$$

where Rg is a noble gas atom. $E_{cmplx}(Rg@C_n)$ is negative if the complexation process is exothermic. Several theoretical computations have been carried out to calculate the complexation energies for the noble gas endohedral complexes of C_{60} and C_{70}.[9−11] For $Rg@C_{60}$, the calculated complexation energies vary with the van der Waals radii of the endohedral atoms. Though there still are some disagreements among theoretical approaches in the relative stability of $Rg@C_{60}$ with respect of the entrapped atoms, it has been generally accepted that C_{60} can be stabilized slightly by a small fraction of an electronvolt upon encaging noble gas atoms.[9] In the case of C_{70}, using the atom−atom potential method, Pang and Brisse found that E_{cmplx} $(Rg@C_{70})$ increases in the order He, Ne, Ar, Xe, and Kr and the larger atoms such as Xe and Kr are too big to be accommodated inside although their complexation energies are more negative.[10] With an approach on the basis of AM1 optimization, however, Sung et al. demonstrated that C_{70} is stabilized in the order He, Ne, Xe, Ar, and Kr.[11] To date there are no experimental data for the complexation energies of $Rg@C_{60}$ and $Rg@C_{70}$ available for comparison with the theoretical. The only experimental approaches that provide an indirect clue to the stabilization of fullerene cages upon encapsulation of noble gas atoms are the binding energies for C_2 loss in the unimolecular decomposition of $Rg@C_{60}^+$.[12] Using the finite heat bath theory (FHBT) and from kinetic energy release distributions (KERDs) in the unimolecular decompositions of $Rg@C_{60}^+$, we have deduced the activation energies for C_2 loss from $Rg@C_{60}^+$ and found that noble gas atoms are shown to stabilize C_{60}. The C_2 evaporation energies increase in the following order: ΔE_{vap} (C_{60}^+), ΔE_{vap} $(Ne@C_{60}^+)$, ΔE_{vap} $(Ar@C_{60}^+)$, and ΔE_{vap}

* To whom correspondence should be addressed. E-mail: bcao@tara.tsukuba.ac.jp (B.C.); james.cross@yale.edu (R.J.C.).
‡ Hebrew University.
† Indiana University. Current address: TARA Center, University of Tsukuba, Japan.
# Yale University.
¶ Deceased.

10.1021/jp0547919 CCC: $30.25
Published on Web 10/21/2005

($Kr@C_{60}^+$), which is in good agreement with the computed stabilization order.[9e]

Determination of KERDs in unimolecular fragmentation provides valuable information on the energetics and dynamics of the reaction. We have carried out the kinetic energy release distribution (KERD) investigations on a series of endohedral fullerene cations. Among the compounds studied were $Ne@C_{60}$, $Ar@C_{60}$, $Kr@C_{60}$, $N@C_{60}$, $N_2@C_{60}$, $N@C_{70}$, $La@C_{82}$, $Tb@C_{82}$, $Ti_2@C_{80}$, $Sc_2@C_{84}$, as well as $Sc_3N@C_{80}$.[6c,7a,12,13] A very recent KERD study is performed on singly and multiply charged $Sc_3N@C_{78}$ and $Sc_3N@C_{80}$.[8] All these endohedral radicals expel C_2 units and undergo cage shrinking in the unimolecular reactions except $N@C_{60}$ and $N@C_{70}$ that, instead, lose the endohedral atom.[7a] The cage-binding energies of these metallofullerenes are extracted from KERDs as well. Yet to the best of our knowledge there is no KERD and cage-binding report on the noble gas atom containing endohedral C_{70}. Here we report the unimolecular decompositions of C_{70}^+ and its noble gas endohedral cations, $Ne@C_{70}^+$ and $Ar@C_{70}^+$. All the three cations lose the C_2 unit in the reaction. The C_2 binding energies in these cations have been deduced from the KERDs. Surprisingly, it is found that introductions of Ne and Ar into C_{70} contribute a little to the stability of C_{70} toward the C_2 loss, which contrasts with the findings in the C_{60} case and in endohedral metallofullerenes.

2. Experimental Section

The production and isolation of C_{70} have been published previously.[14] In brief, the soot containing fullerenes was generated using a dc arc discharge method. A graphite rod (chromatographic grade, ϕ 4.6 × 130 mm, Tokyo Tenso Co.) was vaporized by a dc arc under a 150 Torr flowing He atmosphere. The mixture of fullerenes was extracted from the soot by CS_2 under reflux with protection of Ar for overnight. After removal of the solvent CS_2, the fullerene mixture was dissolved in toluene for high-performance liquid chromatography (HPLC) separation. A PYE column (ϕ 20 × 250 mm; eluant, toluene; room temperature; flow rate, 10 mL/min) was employed for the separation of our target C_{70}. The C_{70} sample thus obtained was confirmed to be free of C_{60} and higher fullerenes by HPLC and mass spectroscopic analyses.

Preparation of $Ne@C_{70}$ and $Ar@C_{70}$ was achieved by doping C_{70} with the noble gases under high pressure at elevated temperature.[6] About 100 mg of pure C_{70} was placed inside an annealed copper tube that is oxygen-free and sealed at one end with a custom-made crimping tool. The open end was attached to a vacuum line using a glass adapter for removal of the air inside the tube and introduction of noble gases into the system. After introduction of Ne (enriched in ^{22}Ne, 70%) and Ar gases, the tube was then cooled in liquid nitrogen and sealed to give an ampule. The ampule was subjected to a high-temperature (650 °C) and high-pressure (3000 atm) treatment in a steel vessel for overnight. The tube, now flattened, was retrieved and cut to remove the solid. C_{70} and its endohedrals were extracted from the solid by CS_2, and about 70 mg of extract was recovered with a doping yield of ~0.2%.

Measurements of parent and its metastable ion peaks were carried out on a high-resolution double-focusing mass spectrometer of reversed geometry, the VG-ZAB-2F, running mass spectra at a very high dynamic range as well as using the technique of mass-analyzed ion kinetic energy (MIKE) spectrometry.[15] Details of the instruments and measurement conditions have been described previously.[7a,12,13] Briefly, the endohedral fullerene cations were obtained by ionization of the corresponding neutral samples that were introduced into the mass spectrometer using a direct insertion probe and evaporated at 400 °C. The electron-impact conditions for ionizing the samples were as follows: electron ionizing energy −70 eV; emission current −5 mA; ion source temperature −400 °C; resolution −1100 (10% valley definition). Metastable ion peak shapes were determined by scanning the electrostatic analyzer and using single-ion counting. Ion counting was achieved by combination of an electron multiplier, amplifier/discriminator, and multichannel analyzer.[16] Combination of the ZAB-2F mass spectrometer with the single-ion counting and with the multichannel analyzer provides a powerful technique that is, because of a very wide range achieved, quite sensitive and allows the detection of even trace amounts of species. This technique was demonstrated to be of great importance in the studies of nonmetallic endohedral fullerenes that are produced in a very low degree of incorporation of the guest species.[6,7,12] Some new endohedral fullerenes, for instance, $HeNe@C_{60}$, $He_2@C_{70}$, $N_2@C_{60}$, $N_2@C_{70}$, $CO@C_{60}$, and $H_2O@C_{60}$, have been found for the first time by use of this technique. The same method was employed here for the detection of $Ne@C_{70}$ and $Ar@C_{70}$. The experiments were performed at 8 kV acceleration voltage and a main beam width of 3−5 V. The data were accumulated in the computer-controlled experiments, monitoring the main beam scan and correcting for the drift of the main beam.[15] Metastable ion peak shapes were the mean values of 100−1000 accumulated scans. The product KERDs were determined from the first derivatives of the metastable ion peak shapes.[17,18]

3. Data Analysis

The mass-analyzed ion kinetic energy (MIKE) spectra for a unimolecular decomposition,

$$Rg@C_{70}^+ \rightarrow Rg@C_{68}^+ + C_2 \qquad (2)$$

reveal the kinetic energy release distributions (KERDs) in the reaction. The KERDs are Boltzmann-like and can be modeled by statistical theories. In a model-free approach developed by Klots,[19a] the KERD is written in the form:

$$p(\epsilon) = \epsilon^l \exp(-\epsilon/k_B T^{\ddagger}) \qquad (3)$$

where ϵ is the kinetic energy release, l is a parameter that ranges from zero to unity depending on the interaction potential between the fragments, k_B is Boltzmann's constant, and $T^{\ddagger}$ is the transition state temperature defined by the average kinetic energy on passing through the transition state. The values of l and $T^{\ddagger}$ can be deduced by fitting the experimental KERDs with eq 3 using nonlinear regression.

The isokinetic bath temperature, T_b, is defined in the finite heat bath theory (FHBT) as the temperature to which a heat bath should be set so that the canonical rate constant, $k(T_b)$, is equal to the microcanonical rate constant, $k(E)$, sampled in the experiment.[19b] T_b is calculated by the following equation:[19a]

$$T_b = T^{\ddagger} C[\exp(\gamma/C) - 1]/\gamma \qquad (4)$$

where C, the heat capacity of the parent ion, is given by $C = 3n - 6$ in units of k_B minus one (n is the number of atoms in the parent ion); γ is the Gspann parameter.[19] The current acceptable value of the Gspann parameter for C_2 loss from fullerene cations[20] is $\gamma = 33$. This γ value has been adopted for the unimolecular decompositions of endohedral fullerene cations.[7a,8,12,13] Here we also employ this γ value for data

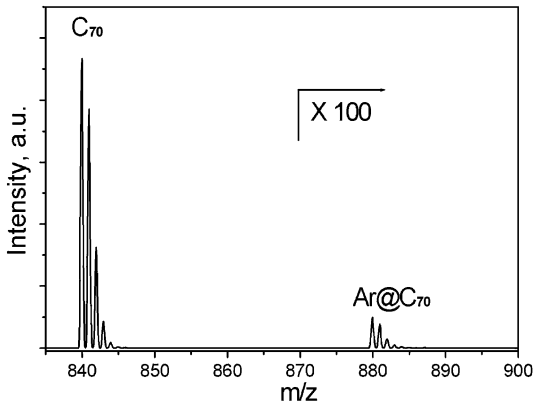

Figure 1. Mass spectrum of a mixture of Ar@C_{70} and C_{70}. The isotopic multiplets beginning at a mass-to-charge ratio of *m*/*z* 880 are from Ar@C_{70}.

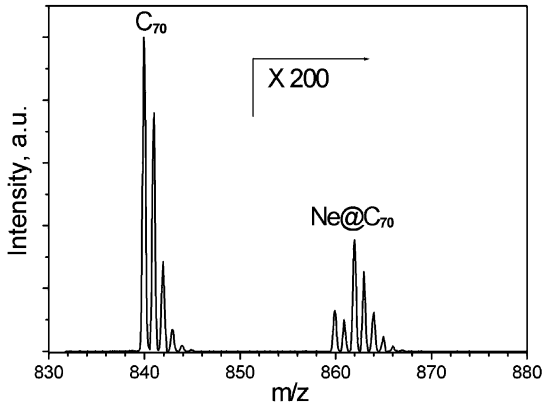

Figure 2. Mass spectrum of a mixture of Ne@C_{70} and C_{70}. The Ne used in this study is enriched with ^{22}Ne (70%). The peaks beginning at a mass-to-charge ratio of *m*/*z* 860 are ascribed to Ne@C_{70} (^{20}Ne@C_{70} and ^{22}Ne@C_{70}).

analysis on the KERDs in the unimolecular reactions of C_{70}^+, Ne@C_{70}^+, and Ar@C_{70}^+.

The binding energies, ΔE_{vap}, for C_2 loss in reaction 2 are calculated from the isokinetic bath temperature, T_b, via the Trouton relation:[7a,8,12,13,20]

$$\Delta E_{vap} = \gamma k_B T_b \quad (5)$$

4. Results and Discussion

4.1. Mass Spectra of Ar@C_{70} and Ne@C_{70}. Presented in Figure 1 is a mass spectrum of the mixture produced by doping C_{70} with Ar under high pressure at elevated temperature. In addition to the peaks that correspond to undoped C_{70}, a series of small but new peaks beginning at a mass-to-charge ratio of *m*/*z* 880 appear in the spectrum. Fitting the relative intensities of these peaks with the natural abundances of ^{40}Ar, ^{12}C, and ^{13}C clearly demonstrates that the peaks at *m*/*z* 880 to ~884 are from the presence of Ar@C_{70}, indicating that the Ar atom has been encapsulated inside C_{70}. The ratio of the filled to the empty C_{70} is seen to be about 0.13%, which is a bit higher than that of its C_{60} analogue.[4]

Illustrated in Figure 2 is a mass spectrum of the mixture of C_{70} and Ne@C_{70}. Similar to the Ar case, some peaks beginning at a mass-to-charge ratio of *m*/*z* 860 are observed together with those of C_{70} in Figure 2. The relative intensities of these peaks are more complicated than those of C_{70} and Ar@C_{70}, whose isotopic peaks are mainly from ^{13}C. Knowing the natural isotopic abundances of ^{12}C and ^{13}C and the isotopic distribution of Ne

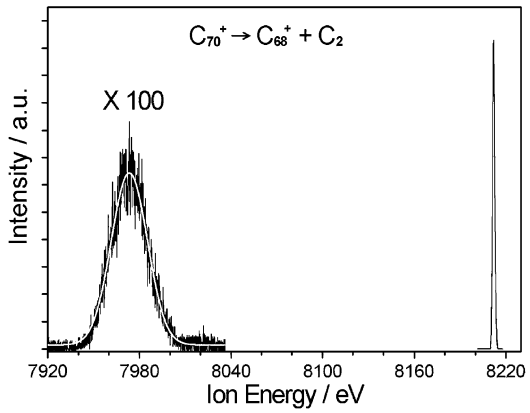

Figure 3. MIKE spectra for unimolecular loss of a C_2 unit from (*m*/*z* 840) C_{70}^+. The narrow peak (right side) is the parent ion C_{70}^+. The broad peak (left side) is the metastable ion C_{68}^+ generated from C_{70}^+ via C_2 loss. The metastable peak is drawn to the same laboratory ion energy scale with its parent peak. The black solid line represents the experimental data, and the white solid line stands for the smoothed spectra obtained by Gaussian fit.

gas used in the study (^{20}Ne/^{22}Ne = 3:7), the relative experimental intensities of the peaks can be fit by the theoretical isotopic distributions of Ne@C_{70} very well, showing the Ne atom has been encaged into C_{70}. The ratio of Ne@C_{70} (^{20}Ne@C_{70} together with ^{22}Ne@C_{70}) to C_{70} in the mixture is about 0.2%, which roughly doubles that of its C_{60} analogue.[4]

4.2. MIKE Spectra and Unimolecular Decompositions of C_{70}^+, Ne@C_{70}^+, and Ar@C_{70}^+. The contribution of ^{13}C in C_{70} together with the isotopes of ^{20}Ne and ^{22}Ne affords isotopic multiplets in the mass spectra of C_{70}^+, Ne@C_{70}^+, and Ar@C_{70}^+, as shown in Figures 1 and 2. It has been verified that the isotopomers of the fullerene cation studied have a significant effect on the shape of the MIKE spectrum and, therefore, on the KERDs and binding energies derived from the MIKE.[8] Careful selection for just one mass among the isotopes of the parent ion is necessary for measurement of the MIKE. A high-resolution double-focusing mass spectrometer of reversed geometry, the VG-ZAB-2F, runs mass spectra at a very high dynamic range and allows a thorough resolution of the isotopic peaks (see Figures 1 and 2), which makes it possible to pick up only one mass of the isotopic multiplets.[15] All the MIKE scans of the parent ions of C_{70}^+, Ne@C_{70}^+, and Ar@C_{70}^+ were performed on the preselected, most naturally intense isotope of the isotopic multiplet of peaks in the mass spectra (see Figures 1 and 2), that is, *m*/*z* 840 for $^{12}C_{70}$, 860 for ^{20}Ne@$^{12}C_{70}$, and 880 for ^{40}Ar@$^{12}C_{70}$. Metastable ion peak shapes were determined by scanning the electrostatic analyzer and using single-ion counting that was achieved by combination of an electron multiplier, amplifier/discriminator, and multichannel analyzer.[16] The shapes of the parent and its metastable ion peaks thus recorded were free of effect from isotopes and were Gaussians. Illustrated in Figures 3−5 are the high-resolution MIKE spectra for unimolecular decompositions of C_{70}^+, Ar@C_{70}^+, and Ne@C_{70}^+ together with their Gaussian fits and corresponding parent peaks. In Figure 3 the metastable peak (ion C_{68}^+, left side) is drawn to the same laboratory ion energy scale with its parent peak (ion C_{70}^+, right side) to disclose their relationship in width. The energy broadening in the laboratory scale for the metastable ion is due to the kinetic energy release in the center-of-mass (CM) scale of the ion's dissociation taking placing in the second field-free region (ff2) of the VG-ZAB-2F instrument. In Figure 4 both the parent and metastable ion peak shapes are expended to demonstrate their Gaussian shapes. The black solid

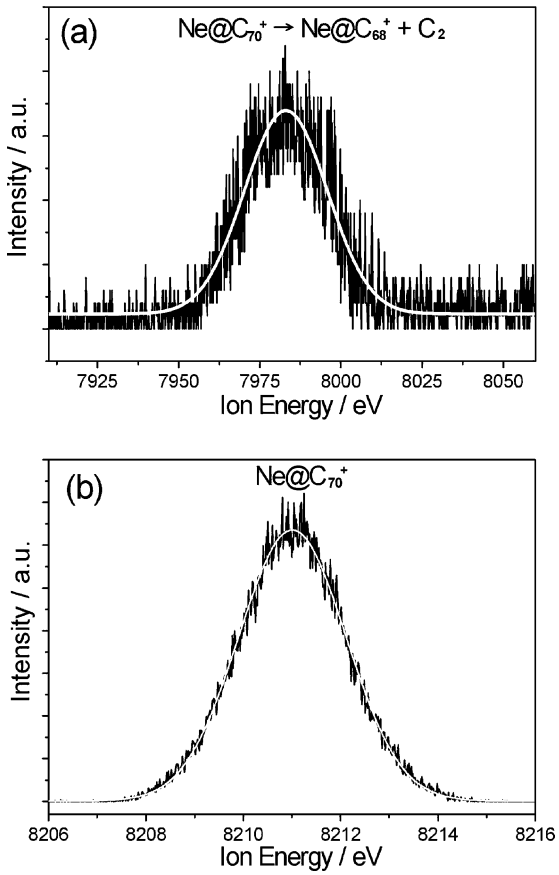

Figure 4. MIKE spectra for unimolecular loss of a C_2 unit from (m/z 860) Ne@C_{70}^+. (a) The metastable ion peak shape. (b) The parent ion peak shape. The black solid lines represent experimental spectra. The white solid lines illustrate the Gaussian fits. Both the parent and fragment ion shapes are clearly seen to be Gaussian.

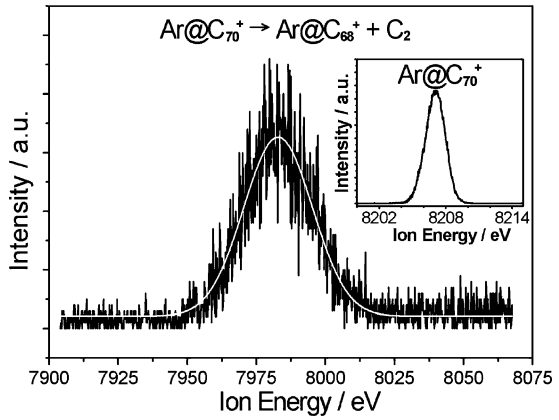

Figure 5. Metastable ion peak shape for unimolecular loss of a C_2 unit from (m/z 880) Ar@C_{70}^+. The precursor ion peak is shown in the inset. Smooth white solid line: Gaussian fit to the experimental spectra (black solid line).

lines represent the experimental data, and the white solid lines stand for the smoothed spectra obtained by Gaussian fit. Both the parent and fragment ion shapes are clearly seen to be Gaussian.

In MIKE spectra the peak position of a daughter ion, U_d, is closely related to that of its parent ion, U_p, by the equation:

$$U_d/U_p = (m_d Z_p)/(m_p Z_d) \tag{6}$$

where m_d and Z_d are the mass and charge of the daughter ion, and m_p and Z_p are the mass and charge of the parent ion. In our current studies both the parent and daughter ions are singly charged ($Z_d = Z_p = 1$). The peak positions deduced by Gaussian fit and corresponding masses of daughter ions calculated using eq 6 are listed in Table 1. The MIKE spectra reveal that C_{70}^+, Ne@C_{70}^+, and Ar@C_{70}^+ cations undergo the following cage-shrinking reactions, also termed as C_2 elimination/evaporation/loss reactions, respectively:

TABLE 1: Peak Positions and Corresponding Masses of Parent and Its Metastable Ions[a]

parent ions	m_p (amu)	U_p (eV)	U_d (eV)	m_d (amu)	$m_p - m_d$ (amu)
C_{70}^+	840	8210	7974	816	24
Ne@C_{70}^+	860	8211	7982	836	24
Ar@C_{70}^+	880	8207	7984	856	24

[a] U_p and m_p (U_d and m_d) are the peak position and mass of parent ion (daughter ion), respectively.

$$C_{70}^+ \rightarrow C_{68}^+ + C_2 \tag{7}$$

$$Ne@C_{70}^+ \rightarrow Ne@C_{68}^+ + C_2 \tag{8}$$

$$Ar@C_{70}^+ \rightarrow Ar@C_{68}^+ + C_2 \tag{9}$$

No evidence for release of the endohedral atoms was detected, and no other fragmentation channels were observed in the unimolecular reactions of C_{70}^+, Ne@C_{70}^+, and Ar@C_{70}^+.

4.3. Kinetic Energy Release Distributions and C_2 Binding Energies in C_{70}^+, Ne@C_{70}^+, and Ar@C_{70}^+. The experimental kinetic energy release distributions (KERDs) were determined from the first derivatives of the metastable ion peak shapes (MIKE spectra) obtained on the preselected masses of parent ions. If the MIKE spectra are Gaussians, the KERDs deduced from both the left and right sides of the spectra will be Boltzmann-like and can be modeled readily by a parameter-free approach using eq 3. The value of l which we found to give the best fit for all the KERDs generated from the Gaussian MIKE spectra is $l = 0.5$. This l value corresponds to the expected value for the most statistical situation, since the translational density of states is proportional[21] to $\epsilon^{0.5}$. This is the case for the present study. The typical center-of-mass product KERDs for reactions 7, 8, and 9 together with the nonlinear regression fits using eq 3 are shown in Figure 6a, b, and c, respectively. The solid lines represent the experimental curves, while the open circles illustrate the fits. The modeled KERDs are superimposed on the experimental ones. The l parameter obtained from the fit curves is 0.50 ± 0.01 for all the three cations, C_{70}^+, Ne@C_{70}^+, and Ar@C_{70}^+. The transition temperatures deduced from KERDs for reactions 7, 8, and 9 are 3326, 3373, and 3435 K, respectively. The average kinetic energy release is calculated via the equation:[7a,8,12,13,20]

$$\epsilon_{av} = (1 + l)k_B T^{\ddagger} \tag{10}$$

where ϵ_{av} is the average kinetic energy release. The binding energies for C_2 loss from C_{70}^+, Ne@C_{70}^+, and Ar@C_{70}^+ deduced from the experimental KERDs are 10.3 ± 0.4, 10.4 ± 0.5, and 10.6 ± 0.5 eV, respectively. All the parameters for the KERDs are listed in Table 2. Under the same conditions the C_2 evaporation energy in C_{60}^+ is measured to be 11.0 ± 0.4 eV, which is much higher than that in C_{70}^+. No destabilization of C_{70} was found upon introduction of Ar and Ne into the cage. No big difference in the C_2 evaporation energy was observed for C_{70}^+, Ne@C_{70}^+, and Ar@C_{70}^+, indicating that incorporations

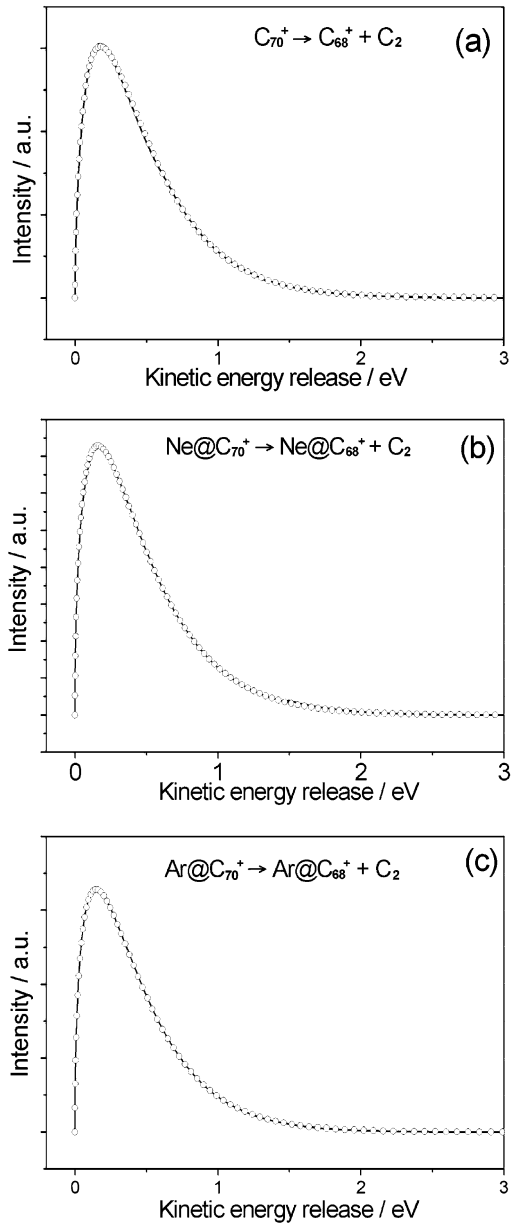

Figure 6. Kinetic energy release distributions (KERDs) in the center-of-mass (CM) system deduced from the metastable peak shapes for reactions (a) $C_{70}^+ \rightarrow C_{68}^+ + C_2$, (b) $Ne@C_{70}^+ \rightarrow Ne@C_{68}^+ + C_2$, and (c) $Ar@C_{70}^+ \rightarrow Ar@C_{68}^+ + C_2$. (Solid line: experimental. Open circle: fit based on eq 3.)

TABLE 2: Transition State Temperatures ($T^{\ddagger}$), Average Kinetic Energy Releases (ϵ_{av}), and C_2 Binding Energies (ΔE_{vap}) Deduced from KERDs Using the Finite Heat Bath Theory and Gspann Parameter $\gamma = 33$'

parent ions	$T^{\ddagger}$ (K)	T_B (K)	l	ϵ_{av} (eV)	ΔE_{vap} (eV)
C_{70}^+	3326	3610	0.50	0.43	10.3 ± 0.4
$Ne@C_{70}^+$	3373	3657	0.50	0.44	10.4 ± 0.5
$Ar@C_{70}^+$	3435	3724	0.50	0.44	10.6 ± 0.5

of Ne and Ar into C_{70} contribute a little to the stability of C_{70} toward C_2 loss, which contrasts with the findings in their C_{60} analogues and in metallofullerenes that the filled fullerenes are substantially stabilized compared with their precursors.[12,13]

4.4. Discussion. We observed here that under similar generation conditions the incorporation yields for $Ne@C_{70}$ and $Ar@C_{70}$ are higher than those for their C_{60} analogues, respectively.[4] This is probably due to the difference in C_2 binding energy between C_{60} and C_{70}. According to the window's mechanism proposed for incorporation and release of a nonmetallic atom,[3] the noble gas atoms were incorporated into fullerene cages by first breaking a bond to open a window in the cage, then entering through the opening, and finally closing the window. The C_2 binding of the fullerene cage provides information on how readily a bond breaks in the cage and therefore furnishes a hint about the easiness for opening the window. The observation that C_{70} is easier to be doped than C_{60} signifies that C_{70} might possess a lower C_2 binding energy than C_{60}. This is the case—the measured C_2 evaporation energy in C_{70} is indeed about 0.7 eV lower than that of C_{60} (see section 4.3 above).

In principle there should be a competition in the unimolecular dissociations of endohedral fullerenes between elimination of an endohedral atom and loss of a C_2 unit from the cage. In what channel the endohedral fullerene cation decomposes depends on the activation energies of the two channels. The fact that no evidence for release of the endohedral atoms was detected in the unimolecular dissociation of $Ne@C_{70}^+$ and $Ar@C_{70}^+$ suggests that the activation energies for loss of the noble gas atom from these cations are higher than those for loss of the C_2 unit, that is, the energy barrier to open a window in the cage for exclusion of the noble gas atom from the fullerene is higher than the barrier for C_2 loss.

Using the atom−atom potential method, Pang and Brisse demonstrated that introduction of Ne and Ar into C_{70} could stabilize the cage by ~0.17 and ~0.39 eV, respectively, and presumed that He, Ne, and Ar could form stable endohedral complexes with C_{70}.[10] Theoretical approaches toward the complexation energies of $Ne@C_{70}$ and $Ar@C_{70}$ by Sung et al.[11] gave almost the same stabilization energies with those by Pang and Brisse. We did observe the difference in the C_2 binding energy for C_{70}^+, $Ne@C_{70}^+$, and $Ar@C_{70}^+$ (see Table 2), but in terms of experimental uncertainties the differences are too small to suggest an obvious stabilization of the cage toward C_2 elimination upon incorporation of the noble gas atoms Ne and Ar into it. It must be pointed out, however, that the stabilities of endohedral fullerenes and their cations might not be necessarily identical, and the difference in the C_2 binding energy between C_{70}^+ and its endohedral cation does not directly equal the value of stabilization energy $E_{cmplx}(Rg@C_n)$ defined in theoretical approaches by Pang and Brisse[10] and by Sung et al.[11] This difference provides an indirect clue to the stabilization of fullerene cages upon encapsulation of noble gas atoms. Our results that the cage-binding energies of $Ne@C_{70}^+$ and $Ar@C_{70}^+$ are not lower than that of C_{70}^+ do indicate introduction of Ne and Ar into C_{70} does not destabilize the cage. This is in agreement with the theoretical predictions by Sung et al. and by Pang and Brisse.[10,11]

It is found that the C_2 binding energy of the C_{60} cage is enhanced upon encaging of the noble gases and increases with the size of the endohedral atom.[12] The C_2 evaporation energy of C_{60}^+ is increased by 0.6 and 0.9 eV for Ne and Ar, respectively, and by as large as 1.6 eV for Kr endohedral (experimental error ±0.4). This is not the case for C_{70}^+ and its endohedrals. Here we found that the C_2 binding energies in C_{70}^+, $Ne@C_{70}^+$, and $Ar@C_{70}^+$ are almost identical within experimental errors. The discrepancy in the effect on C_2 binding upon introduction of noble gas atoms mentioned above between $Rg@C_{60}^+$ and $Rg@C_{70}^+$ is probably in part because of the difference in size between the two cages. While the noble gas atoms fit nicely inside C_{60}^+, one can easily imagine that they will not fit so readily inside C_{58}^+, especially if the isomer of

C_{58}^+ formed by the loss of the C_2 unit is not very spherical, i.e., $E_{cmplx}(Rg@C_{60}^+)$ for reaction 11 is much more negative than $E_{cmplx}(Rg@C_{58}^+)$ for reaction 12:

$$Rg + C_{60}^+ \rightarrow Rg@C_{60}^+ \qquad E_{cmplx}(Rg@C_{60}^+) \quad (11)$$

$$Rg + C_{58}^+ \rightarrow Rg@C_{58}^+ \qquad E_{cmplx}(Rg@C_{58}^+) \quad (12)$$

$$C_{60}^+ \rightarrow C_{58}^+ + C_2 \qquad \Delta E_{vap}(C_{60}^+) \quad (13)$$

$$Rg@C_{60}^+ \rightarrow Rg@C_{58}^+ + C_2 \qquad \Delta E_{vap}(Rg@C_{60}^+) \quad (14)$$

Using reactions 11, 12, 13, and 14, one can deduce relationship 15 among $E_{cmplx}(Rg@C_{60}^+)$, $E_{cmplx}(Rg@C_{58}^+)$, $\Delta E_{vap}(Rg@C_{60}^+)$, and $\Delta E_{vap}(C_{60}^+)$ by forming the thermodynamic cycle:

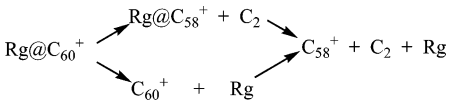

$$\Delta E_{vap}(Rg@C_{60}^+) - \Delta E_{vap}(C_{60}^+) = E_{cmplx}(Rg@C_{58}^+) - E_{cmplx}(Rg@C_{60}^+) \quad (15)$$

Since there is a big difference between $E_{cmplx}(Rg@C_{58}^+)$ and $E_{cmplx}(Rg@C_{60}^+)$ as discussed above, one can find from eq 15 that it is rational that the C_2 evaporation energy, $\Delta E_{vap}(Rg@C_{60}^+)$, for the C_2 loss from $Rg@C_{60}^+$ is larger than that from C_{60}^+ ($\Delta E_{vap}(C_{60}^+)$).

In comparison with C_{60}, however, C_{70} has more room inside for the noble gas atom. If the C_2 is removed from one end of C_{70}, it would not affect the fit very much. In other words, there will be no big difference between $E_{cmplx}(Rg@C_{70}^+)$ for reaction 16 and $E_{cmplx}(Rg@C_{68}^+)$ for reaction 17.

$$Rg + C_{70}^+ \rightarrow Rg@C_{70}^+ \qquad E_{cmplx}(Rg@C_{70}^+) \quad (16)$$

$$Rg + C_{68}^+ \rightarrow Rg@C_{68}^+ \qquad E_{cmplx}(Rg@C_{68}^+) \quad (17)$$

$$\Delta E_{vap}(Rg@C_{70}^+) - \Delta E_{vap}(C_{70}^+) = E_{cmplx}(Rg@C_{68}^+) - E_{cmplx}(Rg@C_{70}^+) \quad (18)$$

Therefore, it is not too surprising that the C_2 binding energies for $Ne@C_{70}^+$, $Ar@C_{70}^+$, and C_{70}^+ are almost identical within experimental uncertainties (see eq 18 deduced in the same way with eq 15).

We have carried out first a preliminary study,[12a] and then very thorough studies,[6c,7a,12,13,20] of the unimolecular decompositions of endohedral fullerene cations using tandem mass spectrometry. Among the compounds studied were $Ne@C_{60}$, $Ar@C_{60}$, $Kr@C_{60}$, $N@C_{60}$, $N_2@C_{60}$, $N@C_{70}$, $La@C_{82}$, $Tb@C_{82}$, $Ti_2@C_{80}$, $Tb_2@C_{84}$, $Sc_2@C_{84}$, as well as $Sc_3N@C_{80}$. Here we added another two new members, $Ne@C_{70}$ and $Ar@C_{70}$, into this family. All these endohedral radicals expel C_2 units and undergo cage shrinking in the unimolecular reactions except $N@C_{60}$ and $N@C_{70}$ that, instead, lose the endohedral atom.[7a] The KERDs were measured for the emission of the C_2 unit from the positive ions of these species as well as of the corresponding empty fullerenes C_{60}, C_{70}, C_{80}, C_{82}, and C_{84}. The binding energies for C_2 loss were extracted from the KERDs using the finite heat bath theory. Different endohedral atoms introduced have distinct effects on the binding of the fullerene cage. There is a pronounced increase in the C_2 elimination energy of C_{82} upon introduction of a La atom into the cage and a further increase upon introduction of a Tb atom.[12a,b,13] Incorporation of two Sc atoms into C_{84} destabilizes the cage binding slightly, whereas two Tb atoms have enhanced the C_2 evaporation energy of the cage.[12a,b] The physical reason for this difference stems probably from the number of electrons transferred within the molecules: it has been proved that four electrons in total have been transferred from the two Sc atoms to the C_{84} cage and the valence state of Sc in $Sc_2@C_{84}$ is +2, whereas the Tb atom is in its +3 valence state, and the electronic structure of $Tb_2@C_{84}$ is $(Tb_2)^{6+}(C_{84})^{6-}$.[12c,d] The C_2 binding energies of C_{80} (D_2 isomer) and $Sc_3N@C_{80}$ (I_h) and $Ti_2@C_{80}$ (D_{5h} and I_h) are identical within experimental uncertainty, indicating that the most unstable I_h and D_{5h} isomers of C_{80} have been stabilized by the clusters Sc_3N and Ti_2 to the level of D_2-C_{80} that is the most stable C_{80} cage.[13] The very reactive atom N, not the C_2 unit, was eliminated in the unimolecular reactions of $N@C_{60}^+$ and $N@C_{70}^+$, suggesting the binding energy for N-loss is lower than that for emission of the C_2 unit.[7a] We found that the contribution of noble gases to the binding energy of C_{70} is much smaller than that in the metallofullerene cases. It is found that upon incorporation of metals the fullerene cages are in general stabilized by an intramolecular electron transfer from the metal to the cage.[22−24] The electron transfer within the molecule generates a positively charged metal core surrounded by a negatively charged carbon cage—the so-called "superatom" structure—and plays a key role in the formation of metallofullerenes.[23] But this is not the case when the noble gases and extremely reactive N atom are involved as guest atoms in endohedrals. Within these nonmetallic endohedral fullerenes no electron transfer occurs, the guest atoms are located at or very close to the center of C_{60} or C_{70}, and the interaction between the endohedral atom and carbon cage is the van der Waals force. Because the van der Waals force between the noble gas atom and C_{60}/C_{70} is much weaker than the ionic bond between the metal ion and the negatively charged fullerene cage of metallofullerene, it is rational that the contribution of encaged metal to the C_2 binding energy of the cage is stronger than that of the noble gas atom. This is probably one of the reasons that the nonmetallic endohedral fullerenes are always produced in low yield.

5. Conclusions

The unimolecular decompositions of C_{70}^+, $Ne@C_{70}^+$, and $Ar@C_{70}^+$ have been studied using tandem mass spectrometry techniques. Information on the energetics and dynamics of the reactions has been extracted. These cations undergo the cage-shrinking reactions via C_2 loss, and no endohedral atom is detected in the reaction. The activation energies for C_2 loss from $Ne@C_{70}^+$ and $Ar@C_{70}^+$ are lower than those for emission of the Ne and Ar atoms. The cage C_2 binding energies determined from the kinetic energy release distributions in unimolecular decompositions of C_{70}^+, $Ne@C_{70}^+$, and $Ar@C_{70}^+$ increase in the order $\Delta E_{vap}(C_{70}^+) < \Delta E_{vap}(Ne@C_{70}^+) < \Delta E_{vap}(Ar@C_{70}^+)$, but no big difference in the cage binding was observed within experimental errors. Inclusion of the Ne and Ar atoms into C_{70} contributes a little to the stability of C_{70} toward C_2 loss. The effect on C_2 binding upon introduction of the noble gas atoms into C_{60} is much larger than that for incorporation of these atoms into C_{70}. This difference is in part because of the discrepancy in size between C_{60} and C_{70}. The contribution of encaging the metallic atom to the stability of the fullerene cage toward C_2 loss is much larger than that of encapsulating the noble gas atom.

Acknowledgment. This research is partially supported by the Hebrew University Intramural Research Fund Basic Project

Awards. We thank the Austrian Friends of the Hebrew University. The work at Yale is supported by the National Science Foundation. The Farkas Research Center is supported by the Minerva Gesellschaft für die Forschung GmbH München.

References and Notes

(1) (a) Weiske, T.; Böhme, D. K.; Hrusäk, J.; Krächmer, W.; Schwarz, H. *Angew. Chem., Int. Ed. Engl.* **1991**, *30*, 884. (b) Weiske, T.; Hrusäk, J.; Böhme, D. K.; Schwarz, H. *Helv. Chim. Acta* **1992**, *75*, 79. (c) Weiske, T.; Wong, T.; Krächmer, W.; Terlouw, J. K.; Schwarz, H. *Angew. Chem., Int. Ed. Engl.* **1992**, *31*, 183.

(2) (a) Saunders, M.; Jiménez-Vázquez, H. A.; Cross, R. J.; Poreda, R. J. *Science* **1993**, *259*, 1428. (b) Saunders, M.; Jiménez-Vázquez, H. A.; Cross, R. J.; Mroczkowski, S.; Freedberg, D. I.; Anet, F. A. L. *Nature* **1994**, *367*, 256. (c) Saunders, M.; Cross, R. J.; Jiménez-Vázquez, H. A.; Shimshi, R.; Khong, A. *Science* **1996**, *271*, 1693.

(3) Becker, L.; Poreda, R. J.; Bada, J. L. *Science* **1996**, *272*, 249.

(4) Akasaka, T.; Nagase, S. *Endofullerenes: A New Family of Carbon Clusters*; Kluwer Academic: Dordrecht, The Netherlands, 2002.

(5) (a) Murata, Y.; Murata, M.; Komatsu, K. *Chem. Eur. J.* **2003**, *9*, 1600. (b) Murata, Y.; Murata, M.; Komatsu, K. *J. Am. Chem. Soc.* **2003**, *125*, 7152. (c) Stanisky, C. M.; Cross, R. J.; Saunders, M.; Murata, M.; Murata, Y.; Komatsu, K. *J. Am. Chem. Soc.* **2004**, *127*, 299. (d) Komatsu, K.; Murata, M.; Murata, Y. *Science* **2005**, 307, 238.

(6) (a) Saunders, M.; Jiménez-Vázquez, H. A.; Cross, R. J.; Mroczkowski, S.; Gross, M. L.; Giblin, D. E.; Poreda, R. J. *J. Am. Chem. Soc.* **1994**, *116*, 2193. (b) Khong, A.; Jiménez-Vázquez, H. A.; Saunders, M.; Cross, R. J.; Laskin, J.; Peres, T.; Lifshitz, C.; Strongen, R.; Smith, A. B. *J. Am. Chem. Soc.* **1998**, *120*, 6380. (c) Peres, T.; Cao, B.; Cui, W.; Khong, A.; Cross, R. J., Jr.; Saunders, M.; Lifshitz, C. *Int. J. Mass Spectrom.* **2001**, *210/211*, 241. (d) Laskin, J.; Peres, T.; Lifshitz, C.; Saunders, M.; Cross, R. J.; Khong, A. *Chem. Phys. Lett.* **1998**, *285*, 7.

(7) (a) Cao, B.; Peres, T.; Khong, A.; Cross, R. J., Jr.; Saunders, M.; Lifshitz, C. *J. Phys. Chem. A* **2001**, *105*, 2142. (b) Knapp, C.; Weiden, N.; Käb, H.; Dinse, K.-P.; Pietzak, B.; Waiblinger, M.; Weidinger, A. *Mol. Phys.* **1998**, *95*, 999. (c) Dietel, E.; Hirsch, A.; Pietzak, B.; Waiblinger, M.; Gruss, A.; Dinse, K.-P. *J. Am. Chem. Soc.* **1999**, *121*, 2432.

(8) Gluch, K.; Feil, S.; Matt-Leubner, S.; Echt, O.; Scheier, P.; Märk, T. D. *J. Phys. Chem. A* **2004**, *108*, 6990.

(9) (a) Son, M.-S.; Sung, Y. K. *Chem. Phys. Lett.* **1995**, *245*, 113. (b) Jiménez, H. A.; Cross, R. J. *J. Chem. Phys.* **1996**, *104*, 5589. (c) Darzynkiewicz, R. B.; Scuseria, G. E. *J. Phys. Chem.* **1997**, *101*, 7141. (d) Patchkovskii, S.; Thiel, W. *J. Chem. Phys.* **1997**, *106*, 1796. (e) Bühl, M.; Patchkovskii, S.; Thiel, W. *Chem. Phys. Lett.* **1997**, *275*, 14.

(10) Pang, L.; Brisse, F. *J. Phys. Chem.* **1993**, *97*, 8562.

(11) Sung, Y. K.; Son, M.-S.; Jhon, M. S. *Inorg. Chim. Acta* **1998**, *272*, 33.

(12) (a) Laskin, J.; Jiménez-Vázquez, H. A.; Shimishi, R.; Saunders, M.; der Vries, M. S.; Lifshitz, C. *Chem. Phys. Lett.* **1995**, *242*, 249. (b) Laskin, J.; Peres, T.; Khong, A.; Jiménez-Vázquez, H. A.; Saunders, M.; Cross, R. J. Lifshitz, C. *Int. J. Mass Spectrom.* **1999**, *185/186/187*, 61. (c) Inakuma, M.; Yamamoto, E.; Kai, T.; Wang, C.; Tomiyama, T.; Shinohara, H.; Dennis, T. J. S.; Hulman, M.; Krause, M.; Kuzmany, H. *J. Phys. Chem. B* **2000**, *104*, 5072. (d) Shi, Z.; Okazaki, T. Shimada, T.; Sugai, T.; Suenaga, K.; Shinohara, H. *J. Phys. Chem. B* **2003**, *107*, 2485.

(13) Peres, T.; Cao, B.; Shinohara, H.; Lifshitz, C. *Int. J. Mass Spectrom.* **2003**, *228*, 181.

(14) Cao, B.; Wakahara, T.; Tsuchiya, T.; Kondo, M.; Maeda, Y.; Rahman, G. M. A.; Akasaka, T.; Kobayashi, K.; Nagase, S.; Yamamoto, K. *J. Am. Chem. Soc.* **2004**, *126*, 9164.

(15) (a) Morgan, P. P.; Beynon, J. H.; Bateman, R. H.; Green, B. N. *Int. J. Mass Spectrom. Ion Phys.* **1978**, *28*, 171. (b) Kirshner, N. J.; Bowers, M. T. *J. Phys. Chem.* **1987**, *91*, 2573.

(16) Lifshitz, C.; Louage, F. *J. Phys. Chem.* **1989**, *93*, 6533.

(17) (a) Holmes, J. L.; Osborne, A. D. *Int. J. Mass Spectrom. Ion Phys.* **1977**, *23*, 189. (b) Lifshitz, C.; Tzidony, E. *Int. J. Mass Spectrom. Ion Phys.* **1981**, *39*, 181.

(18) Jarrold, M. F.; Wagner-Redeker, W.; Allies, A. J.; Kirchner, N. J.; Bowers, M. T. *Int. J. Mass Spectrom. Ion Processes* **1984**, *58*, 63.

(19) (a) Klotz, C. E. *Z. Phys. D* **1991**, *21*, 335. (b) Klotz, C. E. *J. Chem. Phys.* **1989**, *90*, 4470. (c) Klotz, C. E. *Int. J. Mass Spectrom. Ion Processes* **1990**, *100*, 457.

(20) (a) Laskin, J.; Hadas, B.; Märk, T. D.; Lifshitz, C. *Int. J. Mass Spectrom.* **1998**, *177*, L9. (b) Laskin, J.; Lifshitz, C. *Int. J. Mass Spectrom.* **2001**, *36*, 459. (c) Matt, S.; Echt, O.; Sonderegger, M.; David, R.; Scheier, P.; Laskin, J.; Lifshitz, C.; Märk, T. D. *Chem. Phys. Lett.* **1999**, *303*, 379. (d) Lifshitz, C. *Int. J. Mass Spectrom.* **2000**, *198*, 1.

(21) (a) Baer, T.; Hase, W. L. *Unimolecular Reaction Dynamics*; Oxford University: New York, 1996; pp 173−174. (b) Urbain, P.; Remacle, F.; Leyh, B.; Lorquet, J. C. *J. Phys. Chem.* **1996**, *100*, 8003.

(22) (a) Shinohara, H. *Rep. Prog. Phys.* **2000**, *63*, 843. (b) Aihara, J. *J. Phys. Chem. A* **2002**, *106*, 11371.

(23) (a) Cao, B.; Hasegawa, M.; Okada, K.; Tomiyama, T.; Okazaki, T.; Suenaga, K.; Shinohara, H. *J. Am. Chem. Soc.* **2001**, *123*, 9679. (b) Akasaka, T.; Nagase, S.; Kobayashi, K.; Waelchli, M.; Yamamoto, K.; Funasaka, H.; Kato, M.; Hoshino, T.; Erata, T. *Angew. Chem., Int. Ed. Engl.* **1997**, *36*, 1643. (c) Akasaka, T.; Wakahara, T.; Nagase, S.; Kobayashi, K.; Waelchli, M.; Yamamoto, K.; Kondo, M.; Shirakura, S.; Kato, T.; Caemelbecke, E. V.; Kadish, K. M. *J. Am. Chem. Soc.* **2000**, *122*, 9316. (d) Olmstead, M. M.; des Bettencourt-Dias, A.; Duchamp, J. C.; Srevenson, S.; Marcui, D.; Dorn, H. C.; Balch, A. L. *Angew. Chem., Int. Ed.* **2001**, *40*, 1223.

(24) (a) Kobayashi, K.; Sano, Y.; Nagase, S. *J. Comput. Chem.* **2001**, *22*, 1353. (b) Kobayashi, K.; Nagase, S. *Chem. Phys. Lett.* **1998**, *282*, 325. (c) Campanera, J. M.; Bo, C.; Olmstead, M. M.; Balch, A. L.; Poblet, J. M. *J. Phys. Chem. A* **2002**, *106*, 12356.